Finite-size effects for percolation on Apollonian networks

Daniel M. Auto,[1] André A. Moreira,[1] Hans J. Herrmann,[1,2] and José S. Andrade, Jr.[1,2]
[1]*Departamento de Física, Universidade Federal do Ceará, Campus do Pici, 60451-970 Fortaleza, Ceará, Brazil*
[2]*IfB, HIF E12, ETH Hönggerberg, 8093 Zürich, Switzerland*
(Received 4 August 2008; published 23 December 2008)

We study the percolation problem on the Apollonian network model. The Apollonian networks display many interesting properties commonly observed in real network systems, such as small-world behavior, scale-free distribution, and a hierarchical structure. By taking advantage of the deterministic hierarchical construction of these networks, we use the real-space renormalization-group technique to write exact iterative equations that relate percolation network properties at different scales. More precisely, our results indicate that the percolation probability and average mass of the percolating cluster approach the thermodynamic limit logarithmically. We suggest that such ultraslow convergence might be a property of hierarchical networks. Since real complex systems are certainly finite and very commonly hierarchical, we believe that taking into account finite-size effects in real-network systems is of fundamental importance.

DOI: 10.1103/PhysRevE.78.066112 PACS number(s): 89.75.Hc, 64.60.ae, 64.60.ah, 89.75.Fb

I. INTRODUCTION

Complex networks describing real systems are organized in a way that departs from the simple model of a random graph. In their celebrated work, Watts and Strogatz [1] showed for their small-world graphs that a structural parameter, called the cluster coefficient, measuring the formation of groups of three connected neighbors, was much larger than what would be expected in the random regime. It was also observed that some real networks might have a large-scale organization with the presence of communities [2]. Subsequently, these two properties, namely the global organization in communities and the local cluster coefficient, have been brought together in self-similar hierarchical structures where the network is composed of groups within groups [3]. In view of this novel topological concept, techniques of analysis have been proposed to identify the hierarchical construction from the large set of data obtained from real systems [4,5]. A structural organization governing the network topology at all scales is bound to have profound effects on dynamical processes that take place on networks. Such effects are now being revealed by some recent studies [6].

Percolation on complex networks can model a large number of processes in complex systems including, among others, system failure [7] and spreading of epidemics [8]. In this model, one assumes that the network has a fraction p of the edges being present and a fraction $1-p$ of the edges being removed. A surprising aspect of this problem is that in some scale-free network models, global connectivity is kept for any positive probability, $p>0$ [9]. Clearly, this result is only valid in the limit of infinite networks. A natural question therefore arises: How close are real networks from the thermodynamics limit? To answer this question, one needs to develop a finite-size scaling theory for networks, and there has been some effort in this direction [10,11]. However, not much has been done to address this problem taking into account a hierarchical structure of the network.

Here we study the percolation problem on a hierarchical model for complex networks, namely the Apollonian networks. We will investigate two quantities in this problem. The first is the probability of global connectivity, which we define as the probability that two hubs in the networks remain connected after depreciation. We also calculate the fraction of the network occupied by the percolating cluster that connects the hubs. We use renormalization group to find exact renormalization-group equations showing how these quantities vary when we change the scale of the Apollonian network. From this, we are able to show that, in the thermodynamic limit, the critical point is $p_c=0$. However, our scaling relations indicate a very slow, logarithmic, approach to this limit. We suggest that the knowledge of the properties at the infinite size limit may not be representative of what one should expect in real network systems, at least for the case of hierarchical networks.

II. THE APOLLONIAN NETWORK MODEL

The Apollonian networks were inspired by the dense packing of polydisperse spherical grains [12–16]. These networks have a clear geometrical description and their properties are related to the space occupied by the grains. In two-dimensional space, the Apollonian network is a planar graph that is at the same time small-world and scale-free. In higher dimensions, the planarity is lost but the network properties are similar. This limit has been associated to the network of transition paths between local minima in high dimensional rough energy landscapes [17]. Another interesting property of the Apollonian network is that they are intrinsically hierarchical. The way the nodes are connected at small scales provides a possible model for the location of larger groups in a network geometry. Therefore, the network is self-similar, although it cannot be considered as a fractal [5], being rather a pseudofractal [18].

Most of the geometrical properties of Apollonian networks are presented in Ref. [12]. For the sake of completeness we include some of these properties here. The number of nodes in an Apollonian network of nth generation is $N=3+(3^n-1)/2$. These networks exhibit a small world behavior and are scale-free with an exponent $\gamma=1+\ln 3/\ln 2$

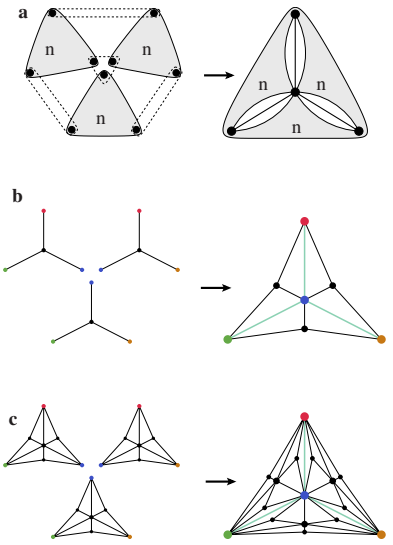

FIG. 1. (Color online) Pictorial representation of the iterative procedure to construct an Apollonian network. (a) Three replicas of the nth generation Apollonian network are merged to form the $(n+1)$th network generation. The gray areas represent the nth generation networks to be merged. The hubs in the corner of previous generation are fused to generate the three corner hubs and the central hub of the following generation. After the merging, three new connections are placed from the center to the corners of the $(n+1)$th network generation. (b) An illustration of the procedure to go from generation 1 to generation 2 of the Apollonian network. The vertex of the same color in each of the three networks of generation 1 is merged into the following second generation. The edges shown in teal are included in the second generation after merging the hub nodes. (c) Three networks of second generation are merged into a third-generation network. The resulting network is identical to the Apollonian network with the exception of the three connections linking the hubs in the corners. This detail has a negligible effect on the results presented here.

≈ 2.585. The cluster coefficient grows with the generation saturating in a value $C \approx 0.828$.

To take advantage of the self-similar structure of the Apollonian network, we use a convenient iterative construction procedure in which we obtain the $(n+1)$th generation from the previous nth network generation. This procedure is illustrated in Fig. 1. We start with three isolated sites in generation 0. At each step three identical replicas of the previous generation networks are connected to each other by direct fusion of hubs, with the central hub of the new generation being merged from the three subnetworks of the previous generation. Finally, three new bonds are added connecting the central hub of the network to each of the hubs at the corners. This procedure generates exactly the Apollonian network, with the three connections linking the corner hubs missing. If desired, these three bonds may be added by hand at the end of the growth procedure. In any event, such a small difference will have a negligible influence on the results presented here. From this procedure, we can find iterative relations between the properties of the network at one scale in terms of the smaller scales. In the case of a perfectly self-similar system, such as Apollonian networks, this renormalization-group approach should provide exact results. Similar techniques have been applied before to solve percolation of complex network models [19,20]. However, to the best of our knowledge, these previous efforts were considered simple cases in which the self-similar parts of the network are connected to the whole system at only two points. Apollonian networks provide a different and more realistic view, since real network communities normally have multiple points of contact with the rest of the system.

III. PERCOLATION

The percolation model on Apollonian networks can be described as follows. After the construction of the network up to nth generation, a fraction of the bonds of the network is removed. The probability of a bond to be retained is given by p, while $q=(1-p)$ is the probability of removal. For this model, we calculate the probability $P_n(p)$ of having a cluster connecting at least two of the hubs in the corners of the network, as well as the fraction of the bonds $M_n(p)$ of such cluster.

Following the iterative construction shown in Fig. 1, we now introduce the renormalization procedure to solve the percolation problem. After the depreciation of the network, there are three possible ways in which the hubs in the corner of the network can be connected to (or disconnected from) each other. First we use the term Y network if the three hubs are connected to each other, and we refer to $M_Y(n)$ and $Y(n)$ as the mass fraction and the probability of finding such a network at generation n, respectively. The second possibility, namely a V network, appears when two hubs of a subnetwork are connected to each other while being disconnected from the third hub. In this case, there are three possible choices for a hub to be disconnected. By symmetry, all three have the same probability V. Here the mass fraction of the cluster connecting the two hubs is $M_V(n)$, while the mass fraction of the cluster connected to the third hub is $M_U(n)$. Finally, the third possibility is an S network, with all three hubs ending up disconnected from each other with probability S. We call $M_S(n)$ the average mass fraction of the cluster connected to the hubs. We can then write the following equation:

$$S = 1 - Y - 3V. \tag{1}$$

In terms of Y, V, and S, the probability $P_n(p)$ is simply given by the sum $P_n(p)=Y+3V$, that is, the total probability of at least two corners of the network being connected.

The renormalization procedure consists of using the probabilities Y, V, S, and p along with the masses M_Y, M_V, M_U, and M_S to obtain expressions for their counterparts in the $(n+1)$th generation network, say Y', V', S', M'_Y, M'_V, M'_U, and M'_S. Exact expressions for Y', V', S' can be obtained in a straightforward, albeit tedious, manner (see the Appendix for details). Here we only quote the final results,

$$Y' = p^3 Y_3 + 3p^2 q Y_2 + 3pq^2 Y_1 + q^3 Y_0,$$

$$V' = p^2 q V_2 + pq^2 V_1 + q^3 V_0,$$

$$S' = 1 - Y' - 3V', \tag{2}$$

where

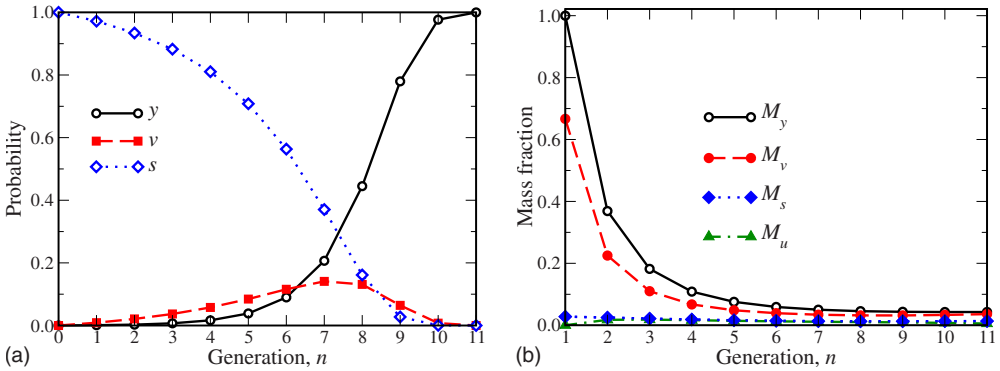

FIG. 2. (Color online) Renormalization for $p=0.1$. (a) Evolution of the percolation probabilities Y, V, and S. We start with the values $Y=V=0$ and $S=1$ at the zeroth generation and iterate Eqs. (2) until the threshold $Y \geqslant 1-10^{-3}$ is reached, which is the adopted convergence criterion (a total of 11 iterations). With this fraction p of bonds present, the probability y for connecting all three corners of the network becomes non-negligible after the sixth iteration. At this point, the mass fraction of the clusters reaches the limiting value of the renormalization process, as can be seen in (b), where we show the evolution for the mass fractions M_Y, M_V, M_U, and M_S. We start with the values $M_Y=M_V=M_U=M_S=0$ at the zeroth generation and iterate Eqs. (2) and (A9). The point $n=0$ has been omitted from (b).

$$Y_3 = 1,$$

$$Y_2 = (Y+2V)(2-Y-2V),$$

$$Y_1 = Y + 4V(Y+2V) + (S-V)(Y+2V)^2,$$

$$Y_0 = Y^2(3-2Y) + 12YV(2V+S) + 3V^2(5V+S),$$

$$V_2 = (V+S)^2,$$

$$V_1 = (2Y+7V)(V+S)^2,$$

$$V_0 = (Y+V)(V+S)^2 + V^2(3V+5S), \tag{3}$$

where Y_3 is the contribution for Y' from situations in which all three of the extra bonds added at the end of the alternate construction procedure remain present after the decimation, Y_2 and V_2 are the contributions when two of them remain present while the third one is removed, and so forth. Equations (2) can be iterated for fixed values of p. Except for $p=0$, this iteration will converge to the only stable fixed point, namely $Y=1$ and $V=S=0$. In other words, we obtain a percolation probability $P_\infty(p)=1$ unless $p=0$, in which case $P_\infty(0)=0$, that is, since our lattice is decomposed randomly, the hubs remain (indirectly) connected in the thermodynamic limit for all positive values of p. This means that the critical point of the percolation transition in Apollonian networks goes to zero, similar to what happens in other scale-free networks [9]. However, as we will demonstrate later, finite-size effects are highly relevant in this system and the behavior in the thermodynamic limit is not representative of what one should expect for networks of sensible scales.

In a similar way as in Eqs. (2) and (3), exact iterative equations can be derived for the mass fractions M_Y, M_V, M_U, and M_S (see the Appendix). By numerically iterating Eq. (A9) along with Eq. (2), we obtain results for the mass fractions and percolation probabilities at different network generations. These results are shown in Figs. 2 and 3 for $p=0.1$ and 0.01, respectively.

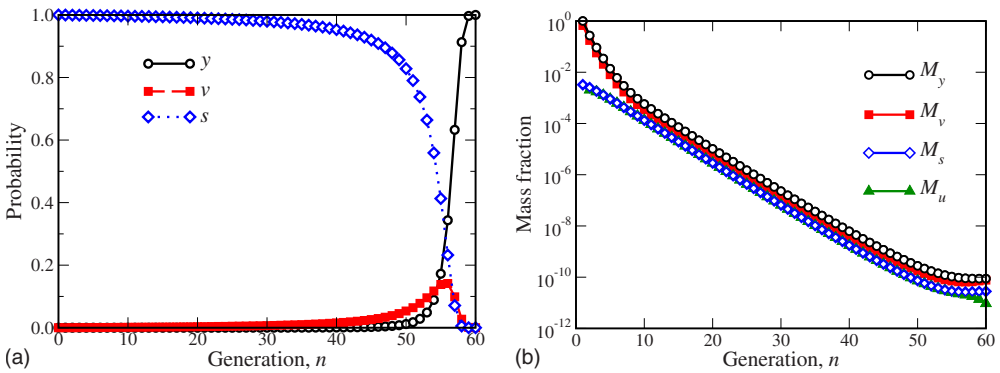

FIG. 3. (Color online) Renormalization for $p=0.01$. (a) Evolution of the percolation probabilities Y, V, and S, obtained by iterating Eq. (2) until the convergence criterion $Y \geqslant 1-10^{-3}$ is met (60 iterations). With this fraction p of bonds, the probability Y only becomes non-negligible after about 55 iterations [compare with Fig. 2(a)]. In (b) we show the evolution for the mass fractions M_Y, M_V, M_U, and M_S, obtained by iterating Eqs. (A9) and (2). Similarly to what can also be seen in Fig. 2(b), these mass fractions converge to a limiting value ($M_Y \sim 10^{-10}$) once the probability Y becomes non-negligible.

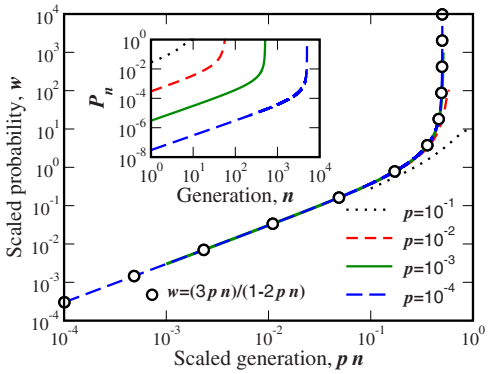

FIG. 4. (Color online) The approach to the thermodynamic limit. The lines correspond to the probability of global connectivity, $P_n=3V+Y$, obtained by numerically iterating Eqs. (2) and (3). In the main panel we show the scaled probability $w=P_n/p$ as a function of the scaled generation pn. One can see that as $p\to 0$, the curves approach the theoretical prediction, Eq. (6). In the inset, we show the original (unscaled) curves.

IV. CRITICAL BEHAVIOR AND FINITE-SIZE SCALING

The results from Figs. 2 and 3 clearly indicate the importance of finite-size effects. In the thermodynamic limit, any probability of occupation p larger than zero should result in a state of global connectivity. However, for the relatively small value of $p=0.1$ this state is not reached before the 6th generation, which corresponds to a network of 367 nodes. For $p=0.01$, the probability of global connection is negligible up the 50th generation, i.e., a network with more than 3.5×10^{23} nodes. In the first generations, while global connectivity is negligible, Y networks appear most likely when two V networks are put together by chance. Due to the symmetry of the problem, there are three ways in which this can happen, and we can therefore approximate $Y\approx 3V^2$. The convergence to the thermodynamic limit is investigated by approximating Eqs. (2) and (3) to a simpler form by considering terms only up to the second order in both p and V,

$$V' = V + 4v^2 + p(4V - 40V^2) + p^2(1 - 15V - 32V^2). \quad (4)$$

We now define the scaled probability $w=3V/p$, and the scaled generation $x=pn$. Replacing the scaled variables in Eq. (4), and making the limit $p\to 0$, we get

$$\frac{dw}{dx} = 3 + 4w + \frac{4}{3}w^2, \quad (5)$$

where we have used $3(V'-V)/p^2=dw/dx$. With the additional condition that $w(0)=0$, we can solve Eq. (5). Identifying w with the scaled probability of global connectivity P_n/p, and restoring our original variables, we arrive at

$$w = \frac{P_n}{p} = \frac{3pn}{1-2pn}. \quad (6)$$

The results shown in Fig. 4 confirm the prediction of Eq. (6).

The obtained scaling shows that the critical occupation fraction, at which global connectivity is reached, approaches zero as the network grows $p_c\sim n^{-1}$. However, this is not a critical exponent in the normal sense. Since the number of nodes of an Apollonian network grows exponentially with the generation, $N=3+(3^n-1)/2$, we have an *ultraslow* convergence to the thermodynamic limit $p_c\sim \ln(N)^{-1}$. This logarithmic convergence has been previously observed in other models such as the bootstrap percolation model [21].

We can now investigate the size of the percolating cluster. Before global connectivity is reached, when one goes from a generation to the next, typically two clusters from the subnetworks merge at the hubs. Since the total size grows by a factor of 3, the mass fraction of the clusters connected to the hubs changes by a factor of 2/3. After global connectivity is reached, the mass fraction does not change with generation since the clusters from all three subnetworks merge into the percolating cluster. We thus conclude that the average mass decreases exponentially with the generation up to a point and then becomes constant, as one can gather from Fig. 3. As a result, it is possible to estimate the average mass fraction by finding at which generation the network becomes globally connected. From Eq. (5) one can see that the probability of global connectivity grows linearly with the generation and then crosses over to an exponential growth when w becomes larger. We then have that the number of generations to reach global connectivity n_c is of the order of $1/p$. The mass fraction of the percolation cluster should then be given approximately by

$$M \sim e^{-\lambda/p}, \quad (7)$$

where λ is constant. This behavior is confirmed by the results shown in Fig. 5. There the mass fraction is plotted as function of $1/p$ as obtained by iterating Eqs. (2) and (A9). We observe the expected behavior. The value that best adjusts this decay is $\lambda\approx 0.242\pm 0.002$. Also in Fig. 5 we present results obtained by numerical simulation of the percolation process in a 14th-generation Apollonian network. The results are in good agreement and follow the expected behavior predicted by Eq. (7).

V. CONCLUSIONS

By applying a real-space renormalization-group technique to the deterministic hierarchical construction of the Apollonian network, we were able to obtain exact iterative equations to compute the probabilities of global connectivity P_n and mass fraction M of the percolating cluster. These equations show that for any positive value of the occupation probability p, this network is always connected in the thermodynamic limit, that is, $p_c\to 0$. We performed simulations of the percolation model for this network and compared the results with those obtained by numerically iterating our equations, and we found them to be in good agreement. By approximating the equations to the limit $p\to 0$, we could also find scaling relations to the critical probability and mass fraction, namely we showed that $p_c\sim n^{-1}$ and $M\sim\exp(-\lambda/p)$, with λ being a constant.

The results presented in this paper provide insight into the problem of percolation on scale-free networks. It is commonly found that scale-free networks are robust to failure [9], meaning that the critical point of percolation gets arbitrarily small for large networks. However, in the case of the

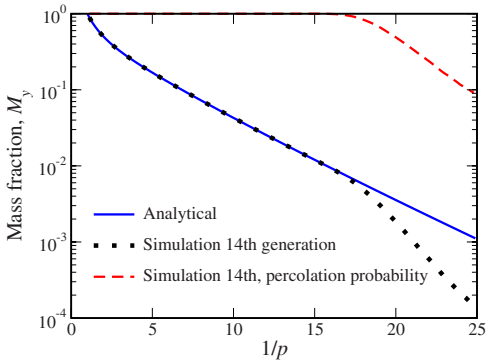

FIG. 5. (Color online) Comparison between analytical and numerical results. The analytical results (blue solid line) are obtained by iterating Eqs. (2) and (A9) for a range of different values of p, until the threshold $Y \geqslant 1-10^{-3}$ is reached, which is the adopted convergence criterion. At this point, the mass fraction occupied by the percolating cluster M_Y reaches a limiting value, as shown in Figs. 2 and 3. This is the average percolating cluster mass fraction for the value of p used. The numerical simulation results (dots) are obtained by applying numerically the percolation model to a 14th generation Apollonian network (7 174 452 bonds). The average is calculated over 10^5 realizations of the model. These two results are in perfect agreement for sufficiently large values of the probability p. For small values of p, finite-size effects of the numerical simulation are no longer negligible and the probability y for the existence of a percolating clusters begins to vanish (red dashed line). This result shows that the fraction occupied by the percolating cluster goes to zero as $\ln(M_Y) \sim -1/p$, that is, the critical transition is of infinite order.

FIG. 6. (Color online) Description of the process to obtain the iterative equations (2). In particular, we show the deduction of the iterative equation for the y probability. The graphical symbols represent how many new connections are added at this iteration (symbols outside the braces) and show the type of subnetwork that is being merged at this iteration (symbols inside the braces). In each case the probability of the corresponding event is presented below the symbol. The probability to obtain a Y network was divided into four different terms. The first term on the right accounts for iterations where three new connections are added. In this case we obtain a Y network, regardless of the type of subnetworks, i.e., this term contributes with p^3. The second term, proportional to $3p^2(1-p)$, accounts for iterations where only two new connections are added. In our pictorial example, we imagine that these connections link the two hubs in the bottom with the hub on top being yet isolated. In this case, to obtain a Y network, the top hub needs to be connected to the rest by the subnetworks. There are two ways in which this can happen, namely either the network on the left connects the hub, and it does not matter what kind of network we have on the right, or the network on the right does not connect the hub, while the one on the left does. The probability for one of these events to happen is represented inside the braces. The other two terms are obtained with similar reasoning.

Apollonian network, its hierarchical structure introduces a number of relevant differences. For instance, although it has an exponent $\gamma \approx 2.56$ for the degree distribution, its critical behavior is quite similar to the marginal case of random networks with $\gamma=3$, where one also finds $M \sim \exp(-\lambda/p)$. This is called an essential singularity and is related to the limit in which $M \sim p^{-\beta}$ with $\beta \to \infty$. Also, the fact that the critical point approaches zero logarithmically shows us that the thermodynamic limit may not be relevant for real hierarchical networks. These two findings are surprising. If the hierarchical structure plays a significant role in the system, not only is the critical condition much larger than what would be expected from the degree distribution, but also the mass fraction is much smaller. The reason for this result is related to the fact that the hubs at each scale are bottlenecks through which the clusters can reach the larger scales. This could be used as a way to devise efficient strategies to increase the system robustness.

ACKNOWLEDGMENTS

This work was supported by the Brazilian agencies CNPq, CAPES, FUNCAP, and FINEP. H.J.H. thanks the Max Planck Society.

APPENDIX

In this appendix, we present the details of our calculations. To obtain the iterative Eqs. (2), we have to find all possible combinations for the three subnetworks being merged. Each subnetwork can be either a Y network, one of the three symmetrically identical V networks, or an S network, resulting in 5^3 different combinations. We must also account for the possible combinations for the three bonds included in the process of going from one generation to the next, as explained in Fig. 1. Since each of the three bonds can be present or not, there are a total of $5^3 \times 2^3 = 1000$ different combinations for the iterative process. By identifying which ones results in Y, V, or S networks in the next generation, we can formulate our iterative equation for the renormalization process. At first this may appear as a rather difficult task, but taking advantage of the symmetry of the network can make it simpler. In Fig. 6, we present a graphical representation of the way we obtained the iterative equation for the probability Y. For other self-similar networks, the same reasoning can be used to derive the iterative equations. This process gets increasingly more complex if one considers that more than three hubs connect the network at different generations. In such cases, one may use a computer to search all the different ways in which the hubs can be connected or disconnected, thus obtaining the renormalization-group relations. We did that in our case in order to get an alternative confirmation of our equations.

After collecting all terms contributing to Y', V', and S', we obtain the expressions for M'_Y, M'_V, M'_U, and M'_S. For instance, if an S subnetwork is merged with two other sub-

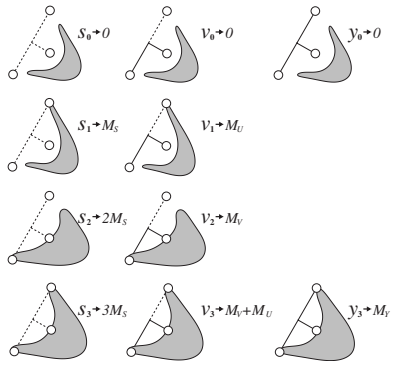

FIG. 7. The auxiliary variable for the computation of the mass fractions. In this picture, the gray area corresponds to a cluster being formed when we go from one generation to the following in the Apollonian network. This cluster can represent a Y, V, or S network, depending on the number of hubs it connects. The empty circles are the three hubs of a subnetwork, which can also be a Y, V, or S network (first, second, and third columns, respectively). In order to compute the contribution of the subnetwork to the mass of the cluster forming in the next generation, we introduce auxiliary variables where the index indicates how many of the hubs of the subnetwork are attached to the forming cluster. Depending on the case, a different mass is added to the cluster, as indicated.

networks to form a Y network, there are two possibilities: either the three clusters of the S subnetwork are connected at the Y network or just two. To account for these two cases, we introduce new auxiliary variables s_2 and s_3 indicating that two or three hubs of the subnetwork are connected to the particular cluster for which we are computing the mass fraction at the following generation. We have then s_3, s_2, s_1, and s_0 as aliases to S; and v_3, v_2, v_1, and v_0 as aliases to V. In each case, the subscript indicates the number of hubs connected to the cluster for which we are computing the mass fraction at the following generation. In the case of the Y networks, either three or none of the hubs are connected to a cluster at the following generation, thus we have y_3 and y_0 as aliases to Y. In Fig. 7, we present a graphical representation of these auxiliary variables. After these contributions have been taken into account, one should set these variables to their appropriate values according to the following definitions:

$$s_0, s_1, s_2, s_3 \to S,$$

$$v_0, v_1, v_2, v_3 \to V,$$

$$y_0, y_3 \to Y. \tag{A1}$$

Under these conventions, Eqs. (3) are rewritten as

$$Y_3 = (y_3 + 3v_3 + s_3)^3,$$

$$Y_2 = (y_3 + 3v_3 + s_3)(y_3 + 2v_3)(y_3 + 4v_3 + 2s_3),$$

$$Y_1 = y_3(y_3 + 3v_3 + s_3)^2 + v_3(y_3 + 2v_3)(3y_3 + 10v_3 + 4s_3) + s_3(y_3 + 2v_3)^2,$$

$$Y_0 = y_3[y_3(y_3 + 9v_3 + 3s_3) + 12v_3(2v_3 + s_3)] + v_2^2(v_2 + 3s_2) + 14v_3^3, \tag{A2}$$

and

$$V_2 = (v_2 + s_2)^2(y_3 + 3v_3 + s_3),$$

$$V_1^{\mathrm{I}} = v_2(v_1 + s_1)^2,$$

$$V_1^{\mathrm{II}} = (y_3 + 2v_3)(v_2 + s_2)^2 + v_2(v_3 + s_3)(v_2 + s_2),$$

$$V_0 = v_2^2 s_3 + v_2 v_3(3v_{\prime}2 + 4s_2) + y_3(v_2 + s_2)^2 + v_2(v_1 + s)^2, \tag{A3}$$

where V_1 has been split as $V_1 = V_1^{\mathrm{I}} + V_1^{\mathrm{II}}$. The reaon for separating these two contributions is to account later for the extra connection added at this generation that may or may not be part of the growing cluster. Since we also need to compute the masses M_U and M_S, the equations for the probabilities S and U need to be written in terms of the new variables,

$$U_2 = (v_1 + s_1)^2,$$

$$U_1^{\mathrm{I}} = v_1(v + s_2)^2,$$

$$U_1^{\mathrm{II}} = (y_0 + 2v_0)(v_1 + s_1)^2 + v_1(v_1 + s_1)(v_0 + s_0),$$

$$U_0 = v_1^2 s_0 + v_2 v_1(v_2 + 2s_2) + 2v_1 v_0(v_1 + s_1) + (y_0 + v_0)(v_1 + s_1)^2, \tag{A4}$$

$$S_1^{\mathrm{I}} = s_1(v_2 + s_2)^2,$$

$$S_1^{\mathrm{II}} = s_1(v_1 + s_1)(v_0 + s_0),$$

$$S_0 = s_0 s_1(2v_1 + s_1) + s_1 v_2(v_2 + 2s_2) + 2v_0 s_1(v_1 + s_1). \tag{A5}$$

Again, the terms U_1^{I}, U_1^{II}, S_1^{I}, S_1^{II} are introduced to account for the cases in which the added connection attaches or not to the cluster. Using Eq. (A1), one returns to the expressions of Eq. (2), and also recovers the relations $U = V$ and $S = 1 - Y - V$.

After rewriting the equations for the probabilities, one can proceed with the calculation of the iterative equations for the mass fractions. Deriving with respect to the auxiliary variables and multiplying by the appropriate mass, we obtain the correct contribution of each term to the mass fraction. With that purpose, we define the set of functions $\bar{X}$ as

$$\bar{X} = \left[yM_y \frac{\partial}{\partial y_3} + v(M_u + M_v)\frac{\partial}{\partial v_3} + vM_v \frac{\partial}{\partial v_2} + vM_u \frac{\partial}{\partial v_1} + 3sM_s \frac{\partial}{\partial s_3} + 2sM_s \frac{\partial}{\partial s_2} + sM_s \frac{\partial}{\partial s_1} \right] X, \tag{A6}$$

where X stands for any of the functions defined in Eqs. (A2)–(A5).

One last point to be taken into consideration is the relative weight of the bonds or nodes in the next generation. The

number of bonds in an nth generation network W_n can be easily calculated as

$$W_n = \frac{3}{2}(3^n - 1), \tag{A7}$$

from which we obtain

$$a = \frac{1}{W_{n+1}} = \frac{2/3}{3^{n+1} - 1},$$

$$b = \frac{W_n}{W_{n+1}} = \frac{3^n - 1}{3^{n+1} - 1}, \tag{A8}$$

where a and b are the relative weight of each of the three new extra bonds added and the weight of each of the three nth generation networks, respectively. As a test, one can verify that $3(a+b)=1$. Putting everything together, we obtain the exact expressions for M'_Y, M'_V, M'_U, and M'_S,

$$Y' M'_Y = p^3 M_{Y_3} + 3p^2 q M_{Y_2} + 3pq^2 M_{Y_1} + q^3 M_{Y_0},$$

$$V' M'_V = p^2 q M_{V_2} + pq^2 M_{V_1} + q^3 M_{V_0},$$

$$V' M'_U = p^2 q M_{U_2} + pq^2 M_{U_1} + q^3 M_{U_0},$$

$$S' M'_S = pq^2 M_{S_1} + q^3 M_{S_0}, \tag{A9}$$

where the mass contributions are given by

$$M_{Y_3} = (3aY_3 + b\bar{Y}_3), \quad M_{Y_2} = (2aY_2 + b\bar{Y}_2),$$

$$M_{Y_1} = (aY_1 + b\bar{Y}_1), \quad M_{Y_0} = (b\bar{Y}_0),$$

$$M_{V_2} = (2aV_2 + b\bar{V}_2), \quad M_{V_1^{\mathrm{I}}} = (b\bar{V}_1^{\mathrm{I}}),$$

$$M_{V_1^{\mathrm{II}}} = (aV_1^{\mathrm{II}} + b\bar{V}_1^{\mathrm{II}}), \quad M_{V_0} = (b\bar{V}_0),$$

$$M_{U_2} = (2aU_2 + b\bar{V}_2), \quad M_{U_1^{\mathrm{I}}} = (aU_1^{\mathrm{I}} + b\bar{V}_1^{\mathrm{I}}),$$

$$M_{U_1^{\mathrm{II}}} = (b\bar{V}_1^{\mathrm{II}}), \quad M_{U_0} = (b\bar{V}_0),$$

$$M_{S_1^{\mathrm{I}}} = (aS_1^{\mathrm{I}} + b\bar{S}_1^{\mathrm{I}}), \quad M_{S_1^{\mathrm{II}}} = (b\bar{S}_1^{\mathrm{II}}),$$

$$M_{S_0} = (b\bar{S}_0), \tag{A10}$$

with $M_{V_1} = M_{V_1^{\mathrm{I}}} + 2M_{V_1^{\mathrm{II}}}$, $M_{U_1} = M_{U_1^{\mathrm{I}}} + 2M_{U_1^{\mathrm{II}}}$, and $M_{S_1} = M_{S_1^{\mathrm{I}}} + 2M_{S_1^{\mathrm{II}}}$. After performing the derivatives, and eliminating the auxiliary variables, we finally obtain

$$M_{Y_3} = 3aY_3 + 3b\{YM_Y + 3V(M_U + M_V) + 3SM_S\},$$

$$M_{Y_2} = 2aY_2 + b\{YM_Y[3 - (V+S)^2] + V(M_U + M_V) \times [9 - 2(V+S) - 3(V+S)^2] + 3SM_S[4 - (Y + 4V + 2S)^2]\},$$

$$M_{Y_1} = aY_1 + b\{YM_Y[1 + 2(Y+2V)(1+V+S)] + V(M_U + M_V) \times [Y(9 - V + 5S) + 12V(2 - V)] + 3SM_S[2Y + 4V(Y+2V) + 3(Y+2V)^2]\},$$

$$M_{Y_0} = 3b\{YM_Y[Y(2-Y) + 4V(2V+S)] + VM_V[Y(4 - Y + 4V) + V(15V + 2S)] + VM_U[Y(4 - Y + 4V) + 14V^2] + SM_S[3Y^2 + 12YV + 2V^2]\}, \tag{A11}$$

$$M_{V_2} = 2a(V+S)^2 + b\{YM_Y[(V+S)^2] + VM_U[3(V+S)^2] + VM_V[2(V+S) + 3(V+S)^2] + SM_S[4(V+S) + 3(V+S)^2]\},$$

$$M_{V_1} = 2a(Y+3V)(V+S)^2 + b\{YM_Y[2(V+S)^2] + VM_U[4(2V + S)(V+S)] + VM_V[(7 - 3Y - 2V)(V+S)] + SM_S[4(2Y+7V)(V+S)]\},$$

$$M_{V_0} = b\{YM_Y[(V+S)^2] + VM_U[V(5V+6S)] + VM_V[2Y(V + S) + 2V(5V+6S) + S^2] + SM_S[4Y(V+S) + V(13V + 2S)]\}, \tag{A12}$$

$$M_{U_2} = 2a(V+S)^2 + b\{VM_U[2(V+S)] + SM_S[2(V+S)]\},$$

$$M_{U_1} = aV(V+S)^2 + b\{VM_V[2V(V+S)] + VM_U[(V+S)^2 + 2(2-S)] + SM_S[4V(V+S) + 2(2Y+5V)]\},$$

$$M_{U_0} = b\{VM_V[2V(V+S)] + VM_U[V(7V+8S) + 2Y(V+S)] + SM_S[2V(4V+S) + 2Y(V+S)]\}, \tag{A13}$$

$$M_{S_1} = aS(V+S)^2 + b\{V(M_V + M_U)[2S(V+S)] + SM_S[3(V+3S)(V+S)]\}$$

$$M_{S_0} = b\{V(M_U + M_V)[2S(V+S)] + SM_S[3V^2 + 12VS + 2S^2]\}. \tag{A14}$$

[1] D. J. Watts and S. H. Strogatz, Nature **393**, 440 (1998).
[2] M. Girvan and M. E. J. Newman, Proc. Natl. Acad. Sci. U.S.A. **99**, 7821 (2002).
[3] E. Ravasz and A.-L. Barabasi, Phys. Rev. E **67**, 026112 (2003).
[4] M. Sales-Pardo, R. Guimerà, A. A. Moreira, and L. A. N. Amaral, Proc. Natl. Acad. Sci. U.S.A. **104**, 15224 (2007).
[5] C. Song, S. Havlin, and H. A. Makse, Nature **433**, 392 (2005).
[6] A. A. Moreira, D. R. Paula, R. N. Costa Filho, and J. S. Andrade, Phys. Rev. E **73**, 065101(R) (2006).
[7] R. Albert, H. Jeong, and A.-L. Barabasi, Nature **406**, 378 (2000).
[8] Y. Moreno, R. Pastor-Satorras, and A. Vespignani, Eur. Phys. J. B **26**, 521 (2002).
[9] R. Cohen, K. Erez, D. ben-Avraham, and S. Havlin, Phys. Rev. Lett. **85**, 4626 (2000).
[10] H. S. Hong, M. Ha, and H. Park, Phys. Rev. Lett. **98**, 258701 (2007).
[11] D.-S. Lee, K.-I. Goh, B. Kahng, and D. Kim, Nucl. Phys. B **696**, 351 (2004).
[12] J. S. Andrade, H. J. Herrmann, R. F. S. Andrade, and L. R. da Silva, Phys. Rev. Lett. **94**, 018702 (2005).
[13] J. P. K. Doye and C. P. Massen, Phys. Rev. E **71**, 016128 (2005).
[14] T. Zhou, G. Yan, and B. H. Wang, Phys. Rev. E **71**, 046141 (2005).
[15] D. J. B. Soares, J. S. Andrade, H. J. Herrmann, and L. R. da Silva, Int. J. Mod. Phys. C **17**, 1219 (2006).
[16] A. P. Vieira, J. S. Andrade, H. J. Herrmann, and R. F. S. Andrade, Phys. Rev. E **76**, 026111 (2007).
[17] C. P. Massen and J. P. K Doye, Phys. Rev. E **75**, 037101 (2007).
[18] S. N. Dorogovtsev, A. V. Goltsev, and J. F. F. Mendes, Phys. Rev. E **65**, 066122 (2002).
[19] S. N. Dorogovtsev, Phys. Rev. E **67**, 045102(R) (2003).
[20] H. D. Rozenfeld and D. ben-Avraham, Phys. Rev. E **75**, 061102 (2007).
[21] M. Aizenman and J. L. Lebowitz, J. Phys. A **21**, 3801 (1988).